

HARPO - A Gaseous TPC for High Angular Resolution Gamma-Ray Astronomy and Polarimetry from the MeV to the TeV

D. Bernard^{a,*}

^aLLR, Ecole Polytechnique, CNRS/IN2P3, 91128 Palaiseau, France

Abstract

We propose a “thin” detector as a high-angular-precision telescope and polarimeter for cosmic γ -rays above the pair-creation threshold. We have built a demonstrator based on a gaseous TPC. We are presently characterizing the detector with charged cosmic rays in the laboratory. Here we present some of its properties.

Keywords: γ -rays, telescope, polarimeter, TPC, pair production, triplet

1. Introduction

Understanding the mechanisms responsible for producing high-energy non-thermal radiation in extreme astrophysical sources, such as AGN and pulsars, relies on having a complete picture of the emission across the EM spectrum.

In practice though, huge sensitivity gaps exist, in particular [1] between the domain of high sensitivity of γ -ray telescopes based of Compton scattering (mainly sub-MeV) and those based on e^+e^- -pair creation (mainly above 100 MeV). Several projects exist to improve the sensitivity of Compton telescopes at the high end of their energy range.

For e^+e^- -pair telescopes, the main obstacle is the degradation of the angular resolution at low energy due to multiple scattering of the conversion electrons : event selection and background rejection become increasingly difficult¹, which ultimately limits the sensitivity.

Furthermore, none of the previous (COS-B, EGRET) or present (FERMI/LAT) e^+e^- -pair telescopes have (had) any significant sensitivity to the polarisation of the incoming photon, a diagnostic that is a powerful tool in the radio, optical and X-ray bands and that is missing for γ -rays. Gamma-rays are emitted by cosmic sources in a variety of non-thermal processes, some of which such as synchrotron radiation or inverse Compton scattering provide linearly polarized radiation to some extent, while others, such as nuclear interactions, end up producing non polarized photons.

Most Compton telescope projects include polarimetry, but the polarization asymmetry of Compton scattering decreases as $1/E$ for $E \gg m_e c^2$, so that Compton polarimetry becomes inefficient above a couple of MeV [2].

2. Thick vs thin detector

The FERMI/LAT, the γ -ray mission presently in space, uses a W/Si converter/tracker followed by a CsI electromagnetic calorimeter : a thick technology for which the effective area is the product of the geometrical area by the efficiency, $A_{eff} = S \times \epsilon$. Over most of the energy range (up to 10 GeV), the angular resolution is dominated by multiple scattering in the tungsten slabs.

In a thin detector [4];

- Only a fraction of the incoming photons are converted, and effective area becomes the product of the cross-section of the conversion process of interest and the sensitive mass, $A_{eff} = \sigma \times M$.

For an argon-based TPC the effective area becomes larger than $1\text{m}^2/\text{t}$ above a couple of MeV (Fig. 1), while the effective area of the three-ton FERMI/LAT plateaus at $\approx 1\text{m}^2$ only above 1 GeV [3].

The energy measurement that is obtained from multiple measurements of multiple scattering of the tracks in the detector at low energy must be complemented by an additional system at higher energy, which will be chosen to be a “thin” system too, so as not to overrun the mass budget, e.g. using a magnetic spectrometer.

- The angular resolution is improved by one order of magnitude (figure 2), and therefore the background rejection factor for point-like sources by two orders of magnitude.
- Polarimetry is performed by analysis of the distribution of the azimuthal angle of the recoil electron in triplet conversion, i.e. the conversion of the incoming photon in the electric field of an electron of the detector, $\gamma e^- \rightarrow e^+ e^- + e^-$. The magnitude of the recoil momentum is typically of the order of MeV/c , the detection of which requires a low density medium.

*On behalf of the HARPO project, LLR Ecole Polytechnique CNRS/IN2P3 and IRFU/CEA.

Email address: denis.bernard at in2p3.fr (D. Bernard)

¹Compare, e.g. the effective area after successive steps in event reconstruction/selection in Fig. 14 of Ref. [3].

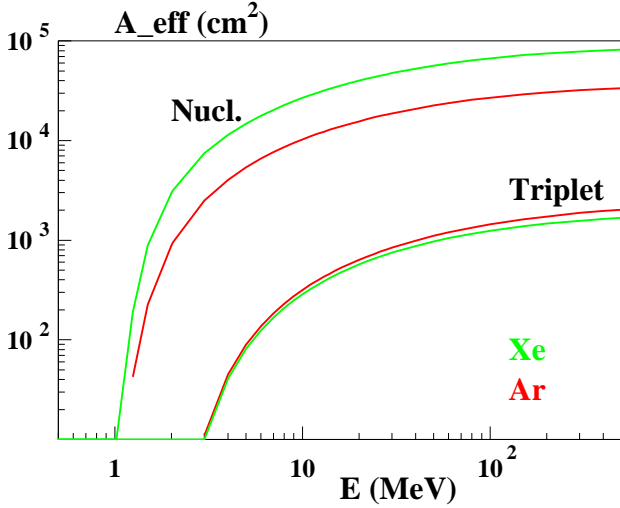


Figure 1: Effective area per ton of sensitive material as a function of the energy of the incoming photon, for nuclear and triplet pair conversion (from Ref. [10]).

A time projection chamber (TPC) i.e., an homogeneous, 3D finely instrumented medium is particularly well suited for such a detection.

3. The demonstrator

We have built a demonstrator consisting of a 5-bar argon-based cubic TPC, with a size of 30 cm, and with a pitch, sampling frequency and diffusion-induced resolution of about 1 mm. The amplification is performed with a “bulk” Micromegas mesh [7], the signal collected by two orthogonal strip sets, and digitized with chips [5] developed for T2K [6].

After we have characterized its performance as a tracker under (charged) cosmic rays in the laboratory, we plan to expose it to a beam of linearly polarized γ rays [8, 9] aiming at:

- validating the technique (γ -ray astronomy and polarimetry).
- obtaining the first measurement of the polarization asymmetries in the low energy part of the spectrum (few-MeV – few 10’s MeV), where the signal peaks, given the spectra of cosmic sources (most often a power law $E^{-\alpha}$, where $\alpha \approx 2$.) and where the polarization asymmetry is rapidly increasing, and where the approximations used in the theoretical calculations (screening, Born approximation) are to be validated².

4. The detector

The layout of the detector is shown on Fig. 3. The TPC uses

²The only experimental validation, to my knowledge, was performed at high energy, and with nuclear pair conversion [11].

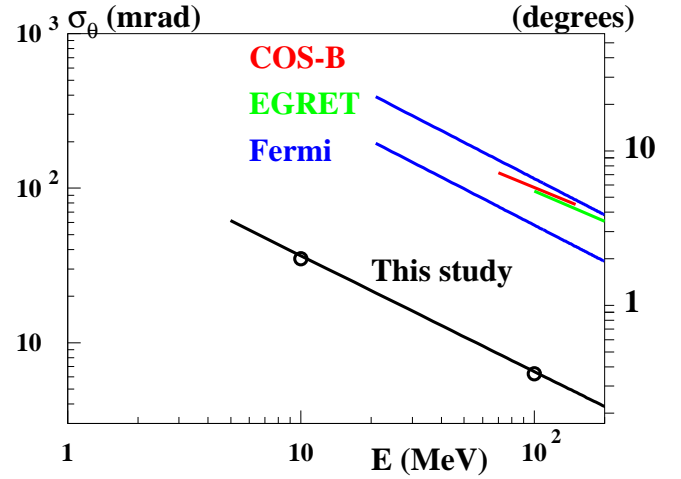


Figure 2: RMS angular resolution as a function of the energy of the incoming photon for a 5 bar TPC, compared to present/past missions (68% containment angle). The Fermi curves (“front” and “back” events) are from the parametrization of Ref. [3].

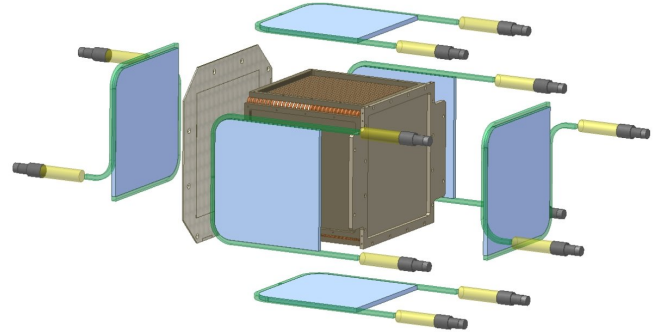


Figure 3: Layout of the detector. The cubic TPC, with the cathode (right) and Micromegas amplification system (right), surrounded by the trigger scintillator plates.

the same argon-based mixture (Ar:95 isobutane:2 CF4:3) as is used by the T2K experiment [6].

The uniform electric field of the TPC is established by a cubic field cage, the side of which are 4 PVC plates, thinned down to 1 mm onto which a kapton foil is glued. The 0.1 mm thick foil is covered by 60 Cu 3mm-wide strips at a pitch of 5mm, with Cu thickness of 35 μ m. A resistance divider is built with a set of pairs of resistances of 10 M Ω , which are paired to an homogeneity of about 3×10^{-4} .

After drift, the ionisation electrons are amplified by a “bulk” Micromegas with a gap of 128 μ m, and collected on a PCB segmented in two series of orthogonal strips, one of which is made of regular copper strips, the other of rectangular pads which are connected by vias to strips lying within the PCB (Fig. 4).

The signal is digitized by an AFTER chip [5], with 72 channels and a range of 12 bits, a shaping time of 100 ns and a maximum sampling rate of 50 MHz, with a maximal number of

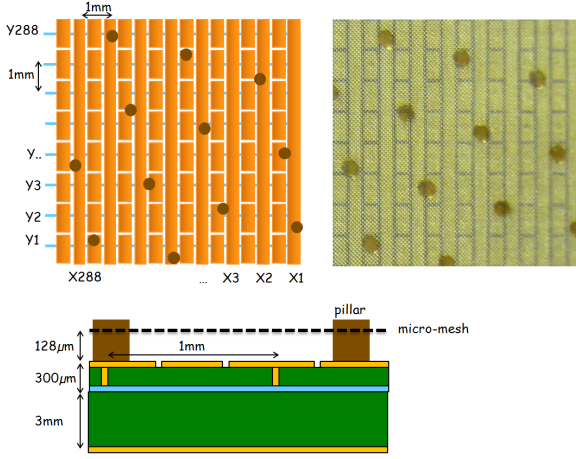


Figure 4: Top : Layout (left) and photograph (center) of the readout. Bottom : Schema of the Micromegas.

time bins of 511. For each transverse direction (x, y), the TPC end plate is instrumented on a width of 288 mm, read by four chips located by one front-end card (FEC) [5]. The electric field is parallel to \vec{z} , so that the third coordinate of a track point in the detector is obtained from the drift time, $z = v_{drift} \times (t - t_0)$.

The trigger is built from the signals from 1 cm thick scintillator plates [12] which surround the TPC (Fig. 3). The scintillation light exiting from the edges of the plates are wavelength shifted in WLS bars. The part of the light that propagates along the bar exits from the pressure vessel and is read by twelve ETL 9125FLB photomultiplier tubes [13].

Data taking can be performed either reading the whole data (“raw”) or after zero suppression (“Zsuppr”) has been applied in the FPGA of the AFTER chip, in which case the digitization time lasts for about 5.5 ms.

Data reconstruction includes thresholding, longitudinal (along one channel) and transverse (at a given bin time) clustering, track reconstruction with a combinatorial Hough method, and matching of the two (x and y) views.

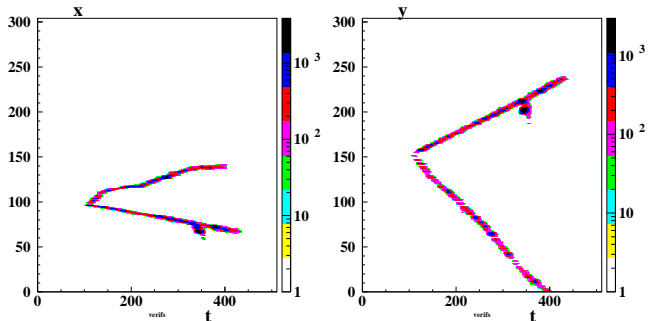


Figure 5: The two views (x, t and y, t) of an event (ADC counts). Units are channel number (x, y), time bin (t).

In cosmic-ray tests most events consist of a simple charged track. Track $x - y$ matching is most easily explained with a

multi-track event, such as that shown on Fig. 5.

The delay of the DAQ was set so that the drift starts at time bin $t = 100$, so we most likely see here the interaction of a cosmic muon (the hard track) with the upper scintillator, producing a delta ray. A softer delta ray is also visible.

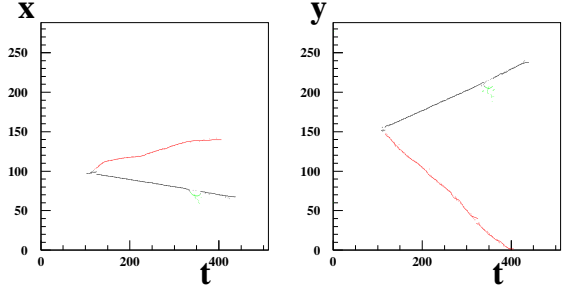


Figure 6: Up : The event shown on Fig. 5 after clustering and track reconstruction. Down : comparison of the x and y time profiles of the three tracks. Units are channel number (x, y), time bin (t).

Track $x - y$ matching is performed, comparing the time distributions of the signal for x and y track. Combinations with the smallest χ^2 are chosen (Fig. 6).

5. Performance

We are presently characterizing the performance of the detector with (charged) cosmic rays in the laboratory. The gas vessel was evacuated to 10^{-4} mbar and then filled with gas from a pre-mixed bottle. Data were collected with the axis of the detector in the vertical position (with the micromegas at the top) : the calibration of the starting time t_0 and drift velocity v_{drift} of the TPC was simply provided by through tracks (Fig. 7).

The study of the variation of the squared RMS cluster size as a function of drift time can provide an estimate of the diffusion of the electron cloud during the drift. In the transverse direction, from the linear variation of σ_T^2 with t for close-to-vertical tracks ($|\theta| < 0.1$ rad), (Fig. 8 left), we obtain a transverse diffusion coefficient of $224 \mu\text{m}/\sqrt{\text{cm}}$, compatible with the Garfield simulation. In the longitudinal direction (right), the shaping of the signal is the dominating effect.

From approximately straight, x/y matched tracks, we obtain a map of the gain homogeneity by dividing the distributions of the position of their clusters weighted by the cluster total measured charge, by the unweighted distribution (Fig. 9).

Finally, an estimate of the spatial resolution is obtained using a four-segment method. After a loose preselection of x/y

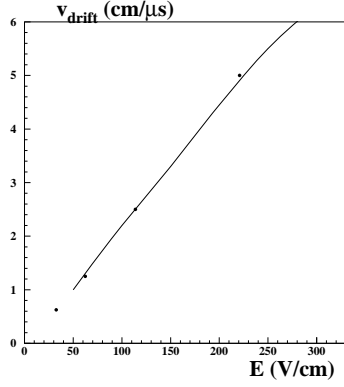


Figure 7: Variation of the drift velocity v_{drift} with the applied electric field, at a gas pressure $P = 2$ bar. Dots : measurements. Curve : Garfield simulation [14].

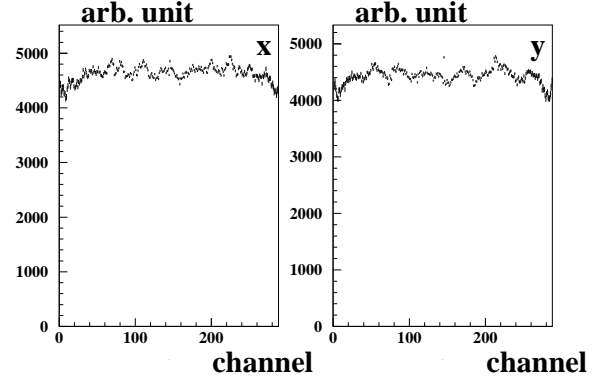


Figure 9: Map of the gain homogeneity. Left : x; Right : y.

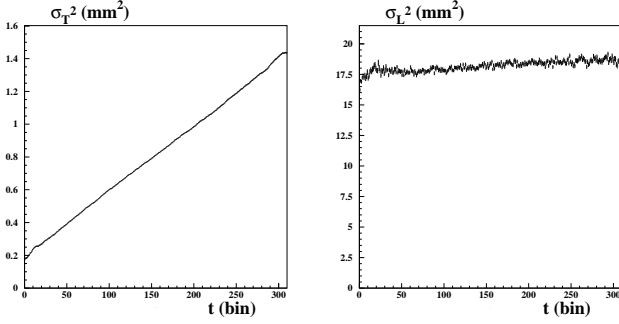


Figure 8: Variation of the squared RMS cluster size in the transverse (left) and longitudinal (right) direction, as a function of drift time ($P = 2$ bar, $E_{drift} = 234$ V/cm).

matched tracks, the track is split into four segments of equal length. Straight tracks are then selected by applying a cut on the extrapolation at the track middle from the two external segments 1 and 4. This does not bias the two internal segments, 2 and 3, the extrapolations of which are compared. We obtain a resolution per segment of $200/\sqrt{2} = 140\mu\text{m}$ in the transverse plane (x or y , Fig. 10).

6. Conclusion

We have built a demonstrator for a TPC-based high-angular-resolution and polarization-sensitive telescope for γ rays above the pair creation threshold. Aspects of its performance for tracking, obtained from cosmic-ray tests in the laboratory, have been presented. We expect to expose this detector to beams of polarized γ ray, to characterize its properties as a γ -ray telescope and polarimeter, and to perform the first measurement of the polarization asymmetry for triplet conversion at low energy.

References

- [1] V. Schoenfelder, *New Astr. Rev.* **48** (2004) 193.
- [2] *New Astronomy Reviews*, **48**, 2004, 215, M. L. McConnell, J. M. Ryan

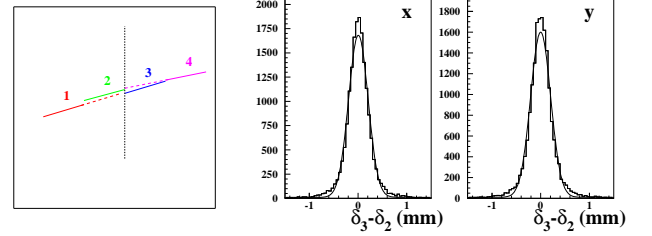


Figure 10: Left : Schema of the 4-segments method. Right : Distribution of the difference in the transverse direction of the extrapolation of segment 2 and 3 to the center of the track.

- [3] Fermi-LAT Collaboration, arXiv:1206.1896 v1 [astro-ph.IM].
- [4] D. Bernard and A. Delbart, *Nucl. Instrum. Meth. A*, In Press, arXiv:1203.5889 [astro-ph.IM].
- [5] P. Baron *et al.*, *IEEE Trans.Nucl.Sci.* **55**:1744-1752, 2008.
- [6] N. Abgrall *et al.*, *Nucl. Instrum. Meth. A* **637**, 25 (2011).
- [7] I. Giomataris *et al.*, *Nucl. Instrum. Meth. A* **560**, 405 (2006)
- [8] S. Amano *et al.*, *Nucl. Instrum. Meth. A* **602** 2009 337
- [9] N. Muramatsu [LEPS Collaboration], arXiv:1201.4094 [physics.ins-det].
- [10] “XCOM: Photon Cross Sections Database”, M.J. Berger *et al.*, NIST.
- [11] C. de Jager *et al.*, *Eur. Phys. J. A* **19**, S275 (2004)
- [12] EJ-208 scintillator, EJ-280 wavelength shifter, Eljen Technology.
- [13] I. Adam *et al.* [BABAR-DIRC Collaboration], *Nucl. Instrum. Meth. A* **538**, 281 (2005).
- [14] R. Veenhof, *Nucl. Instrum. Meth. A* **419**, 726 (1998).